

1 **A long-term hydrological modelling of an extensive green roof**
2 **by means of SWMM**

3 Sara Simona CIPOLLA^a, Marco MAGLIONICO^a, Irena STOJKOV^b

4
5 *^aDepartment of Civil, Chemical, Environmental and Materials Engineering, University of Bologna, Viale*
6 *del Risorgimento 2, 40136 Bologna, Italy.*

7 *^bKleinfelder Northeast, Inc., 215 First Street, Suite 320, Cambridge, MA 02142, USA.*

8 **Corresponding author: Tel.: +39 051 2093354. E-mail address: sara.cipolla@unibo.it (S.S. Cipolla)*

9
10 **ABSTRACT**

11 Green roofs provide multiple environmental and social benefits, among which the
12 opportunity to control storm water runoff as they limit the rate of runoff after urbanization
13 to the rate that would have occurred before urban development. The hydrological
14 behavior of a green roof is site specific, thus the local environmental parameters, the
15 characteristics of the vegetation and the physical properties of its layers have to be
16 considered in the evaluation of its performance. Furthermore, the hydrological
17 performance of a green roof is influenced by the size of the plot (full-scale vs small scale),
18 by the definition of "event", and by the number of events included in the research. From
19 this broader context this paper first provides a review of the scientific literature, with a
20 focus on the hydrological behaviour of experimental full-scale installations and on
21 hydrological modelling of green roof performance. Second, the study presents the results
22 of a monitoring activity of a full-scale extensive green roof in Bologna (Italy). Continuous
23 weather data and runoff were collected between January and December 2014, resulting

24 in 69 storm events suitable for the study. Experimental data show that single event rainfall
25 attenuation ranged from 6.4% to 100% with an annual average value of 51.9% which is
26 consistent with other author's findings. Last, the study uses the field data to calibrate and
27 validate a numerical model realized with the commercial software SWMM 5.1. The
28 model was used to simulate the long-term hydrologic response, over one year, of the same
29 full-scale extensive green roof and to compare it to an adjacent impervious roof of the
30 same size. Modelling results confirm the role of green roofs in restoring the natural water
31 regime by reducing the annual runoff volume. The comparison of the results between the
32 experimental green roof monitoring and the SWMM simulation proved that the suggested
33 model has good capabilities in simulating the hydrograph of stormwater runoff from
34 green roofs along the year, as demonstrated by the quite high values of NSE and the low
35 value of RSR in both the calibration and validation phase. Furthermore, the low difference
36 (< 9%) in total retention between the 69 measured and simulated events confirms the
37 suitability of the model for long term simulations. The proposed modelling approach
38 demonstrates that SWMM can be used for assessing the performance of LID systems
39 (Low Impact Development), and consequently for supporting local authorities or
40 designers in the evaluation of the hydrological efficiency of green roofs.

41 **KEYWORDS**

42 Green roof; LID, modelling; retention; stormwater management; SWMM*

* **Abbreviations:** BRC-LID: “Bio-Retention Cell” LID Type; ET_0 : potential evapotranspiration, ET_r : real evapotranspiration; GR: Green Roof; LID: Low Impact Development; GR-LID: “Green Roof” LID Type; NSE: Nash–Sutcliffe Efficiency index;

43 INTRODUCTION

44 A green roof (GR) is an extension of an existing or newly constructed roof which
45 incorporates a multi-layer structure (water proofing membrane and root barrier, a filter, a
46 drainage system and lightweight growing medium) and plants. The growing popularity
47 of GRs in sustainable buildings is mainly due to their multiple environmental and social
48 benefits (Bianchini and Hewage, 2012; Vijayaraghavan, 2016), among which the
49 hydrological ones. It is repeatedly documented that GRs are a valid tool to restore the
50 hydrological urban water balance by reducing and delaying stormwater runoff (Czemiel
51 Berndtsson, 2010; Palla et al., 2010; Stovin et al., 2015, 2012). Furthermore, a GR acts
52 as a Source Control technology (SC) providing a stormwater management opportunity in
53 otherwise unused spaces: the rooftops. (Fassman-Beck et al., 2013; Fletcher et al., 2014;
54 Versini et al., 2015). As a result, quantifying and improving the hydrological performance
55 of a GR system is becoming increasingly important for stormwater engineers, architects
56 and urban planners (Berardi et al., 2014; Czemiel Berndtsson, 2010; Fassman-Beck et al.,
57 2013; Gambi et al., 2011; Lucas and Sample, 2015; Mentens et al., 2006; Stovin et al.,
58 2012; Voyde et al., 2010b).

59 Stovin et al. (2012) clearly identified the key hydrological mechanisms operating within
60 a GR; they could be summarized in: rainfall interception by leaves, infiltration and
61 retention in the substrate, storage in the drainage layer, and runoff from the detention
62 storage. Any excess of water, above retention capacity, is directed from the drainage layer

RMSE: Root Mean Square Error; RR: Reference roof; **RSR: RMSE-Observation
Standard deviation Ratio**; SC: Source Control technology; SR: Sedum Roof.

63 towards the downspouts, while retained water may subsequently leave the roof as
64 evapotranspiration (Stovin et al., 2015). For improving the retention capacity, which to
65 date is the most cited hydrological performance metric of a GR, a complete knowledge
66 of these mechanisms is needed. Moreover, those processes must be carefully modelled to
67 provide a valid prediction tool for stormwater engineers and municipalities in the design
68 and verification phase, respectively.

69 Furthermore, in the past few years, due to a growing number of research studies (e.g.
70 Blank et al., 2013; Li and Babcock, 2014; for an overview) which demonstrate the
71 effectiveness of GRs from an ecological, social, and economical point of view, the local
72 regulations of many countries have begun to suggest GRs for many purposes, such as
73 urban stormwater management and urban heat island mitigation technologies. She and
74 Pang (2010) underlined how many European countries and local governments in the
75 United States are providing stimulus programs to promote GRs installation by private
76 buildings owners. This is mainly due to the fact that GRs should be considered as a
77 technology for providing an “all round” contribution as part of sustainable development
78 and resilience strategies. This concept has been deemed essential by the European
79 Commission through the HORIZON 2020 research program. At the moment the
80 European Commission promotes research activities “focused on providing evidence that
81 re-naturing of cities through the deployment of innovative, locally adapted, systemic
82 solutions - that are inspired and supported by nature - can be a cost-effective and
83 economically viable way to make cities more sustainable, resilient, greener, and healthier
84 (European Commission, 2015).

85 Currently, several Italian regional and local regulations (as in the Autonomous Province
86 of Bolzano, the Province of Rimini and in the city of Bologna through the Urban

87 Municipal Regulation, RUE) promote the use of GRs and other green technologies,
88 because of their hydrological and environmental benefits, providing incentives such as
89 extra building volumes or extra tax deductions (Bertocchi et al., 2011; Cipolla et al.,
90 2016). It has therefore become essential to identify a method for forecasting the
91 hydrological performance of GRs especially in order to fairly distribute such incentives.

92 **1.1 Overview of the retention performance of full-scale green roofs**

93 Several studies evaluated the hydrological performance of GRs through field monitoring
94 activities, and their results have been compared by other authors through detailed
95 overviews (Czemiel Berndtsson, 2010; Palla et al., 2010; Stovin et al., 2012). However,
96 these authors frequently reported and compared the performance of GRs in terms of
97 average annual retention without taking into account the possible differences between
98 studies conducted on a pilot scale or on a full roof scale. Pilot scale studies are based on
99 elevated test beds or similar modules, with a watershed area that can range between 0.37
100 and 12 m² (Carson et al., 2013), while full-scale GRs typically occupy bigger watershed
101 areas and include non-vegetated regions, which are generally required for maintenance,
102 rooftop equipment, egress or load restrictions. Furthermore, the pilot test beds are
103 frequently elevated above the base level (Beecham and Razzaghmanesh, 2015; Stovin et
104 al., 2015, 2012) while full-scale installations lay on the rooftop. This means that in the
105 last case, the GR's contact with the atmosphere is restricted to the vegetation-air interface
106 while in the first case the bottom surface is usually not protected from weathering. These
107 differences, at the moment not fully investigated, may be the cause of inaccuracies when
108 comparing the overall retention of pilot test beds with full-scale installations. Moreover,
109 considering that not only the physical configuration but also other parameters could

110 influence the average retention (e.g. number of events, definition of events, climatic
 111 condition at the study site, green roof type etc.), to reduce the inaccuracy from the
 112 comparison between full-scale vs pilot green roof, from this point forward only studies
 113 based on retention data provided by experimental studies on full-scale installations will
 114 be taken into consideration.

115 Carson et al. (2013) proposed a detailed review of the hydrologic studies on full-scale GR
 116 systems, in both entire and partitioned sections of occupiable building rooftops. This
 117 review, updated with the results from the latest studies, is summarized in Table 1 and
 118 shows that the retention volume can range from 11.0 % to 76.4 %, which is generally
 119 lower than what reported for pilot test (Stovin et al., 2012). This is probably due, as
 120 underlined by Carson et al., (2013) and work undertaken at Pennsylvania State University
 121 (Berghage et al., 2007), to the presence of a gravel edge or non-vegetated sections and
 122 irrigation requirements for many full-scale systems. Moreover, the presence of air and of
 123 direct solar radiation to which many pilot test boxes are subject to on their bottom face,
 124 may influence the evapotranspiration process and consequently the overall hydrological
 125 performance (higher diurnal soil moisture loss).

Year	Authors	Study Location	Period [mm/yy-mm/yy]	Area [m ²]	Events	Substrate depth [cm]	Ret. [%]
2003	Hutchinson et al. (2003)	Portland, OR	1/02-4/03	240	NA	100-125	69.0
2005	Liu and Minor (2005)	Toronto, CA	3/03-11/04	200	NA	75	57.0
		Toronto, CA	4/03-11/04	200	NA	100	57.0
2005	Moran et al. (2005)	Goldsboro, NC	4/03-9/04	35	67	75	63.0
		Raleigh, NC	7/04-9/04	65	13	100	55.0
2005	Connelly et al. (2005)	Vancouver, CA	1/05-12/05	33	NA	75	29.0
		Vancouver, CA	1/05-12/05	33	NA	150	26.0
2007	Teemusk and Mander (2007)	Tartu, EE	8/04-9/04	120	3	100	19.6
2008	Berkompas et al. (2008)	Seattle, WA	2/07-12/07	743	NA	150	30.5

		Seattle, WA	4/07-6/07	1860	NA	100-125	33.0
		Seattle, WA	10/07-12/07	80	9	150	17.1
2008	Collins et al. (2008)	Goldsboro, NC	4/03-6/04	35	NA	75	64.0
2008	Kurtz Tim (2008)	Portland, OR	5/02-6/08	246	NA	125	56.0
		Portland, OR	3/07-6/08	465	NA	75	64.0
2008	Spolek (2008)	Portland, OR	10/04-4/07	290	NA	100-150	12.0
		Portland, OR	10/04-4/07	280	NA	100-150	17.0
		Portland, OR	1/05-10/07	500	NA	150	25.0
2009	Berghage et al. (2009)	Chicago, IL	8/07-7/09	7000	106	76	74.0
	Bliss et al. (2009)	Pittsburg, PA	8/06-1/07	330	13	140	21.8
2010	Palla et al. (2010)	Genova, IT	5/07-12/08	170	19	200	51.5
2010	Voyde et al. (2010a)	Auckland, NZ	10/08-10/09	41	91	50	66.0
		Auckland, NZ	10/08-10/09	13	91	50	66.0
		Auckland, NZ	10/08-10/09	46	91	70	66.0
		Auckland, NZ	10/08-10/09	45	91	70	66.0
		Auckland, NZ	10/08-10/09	12	91	70	66.0
		Auckland, NZ	10/08-10/09	38	91	50	66.0
2011	Gregoire and Clausen (2011)	Storrs, CT	12/09-2/10	307	NA	102	51.4
2013	Carson et al. (2013)	New York, NY	06/11-06/12	310	74	32	36.0
		New York, NY	06/11-06/13	390	108	100-200	47.0
		New York, NY	06/11-04/14	940	61	100	61.0
2013	Speak et al. (2013)	Manchester, UK	09/11-10/12	408	254	170	65.7
2014	Hakimdavar et al. (2014)	New York, NY	08/11-1/12	310	113	32	50.6
		New York, NY	8/11-06/12	99	110	32	61.3
2014	Yang et al. (2015)	Beijing, CN	04/12-7/12	120	13	150	76.4
2015	Versini et al. (2015)	Paris, FR	06/11-8/12	35	100	30	17.0
		Paris, FR	06/11-8/12	35	100	150	11.0

126 **Table 1.** Summary of studies on the hydrological performance of full-scale GRs. Columns from left to
127 right identify: year of publication, authors reference, geographic location of the site, time period of data
128 collection, size of the monitored drainage area, number of individual events observed, depth of the
129 growing substrate, and average retention during the monitoring period for each study. The symbol NA is

130 used for fields where information was unavailable.

131 It should be noted that not only the size of GRs (full-size vs pilot) but also other factors
132 such as the definition of the term “event”, the number of considered events, the climatic
133 conditions, the substrate depth and composition, and last but not least the vegetation
134 planted, have a notable influence on the average retention of a GR. The definition of the
135 term "event" strongly influences the retention and consequently the performance of a
136 green roof as source control technology. In some previous studies the individual events
137 were defined as being separated by continuous dry periods of at least six hours (Stovin,
138 2010; Stovin et al., 2013, 2012). For others, events were independent if separated by at
139 least one hour of dry weather time (Locatelli et al., 2014) and a few studies did not define
140 the minimum dry weather time before each event (Teemusk and Mander, 2010; Yang et
141 al., 2014). When the antecedent dry weather time increases, small events (with retention
142 equal to 100%) are embedded in the previous events, and this may cause the reduction of
143 the overall retention of the roof. To contrast this ambiguity in the event definition, some
144 manuscripts provide a detailed description of the procedure used for the data analysis
145 (climate, number of events, rainfall depth) and on top of that, they provide a definition of
146 events that take into account both precipitation and runoff (Carson et al., 2013;
147 Hakimdavar et al., 2014). In particular, for those authors a storm event begins when
148 rainfall is first recorded and ends when no precipitation or runoff has been recorded for
149 at least 6 hours.

150 That being said, it is clear how the absence of common standards, for collecting and
151 analysing data, determines a significant difficulty in the comparison of experimental
152 results coming from different research activities. To overcome this, in this study the
153 methodology used for event definition and data analysis, followed the procedures used

154 by Carson et al. (2013) and by Hakimdavar et al. (2014) to analyze the hydrological
155 behaviour of some full-scale GRs in New York City (USA). The aim is to develop and
156 follow common standards for data recording and analysis, allowing at the same time an
157 easier and better comparison of the results.

158 **1.2 Overview of the hydrological models**

159 In the last few years, researchers have proposed empirical relations between rainfall and
160 runoff based on field experiments (Carson et al., 2013; Fassman-Beck et al., 2013), event-
161 based hydrological models (Bengtsson et al., 2005; Carbone et al., 2014; Jarrett et al.,
162 2006; Kasmin et al., 2010; Lamera et al., 2014; Palla et al., 2012; She and Pang, 2010),
163 conceptual models for long term simulation (Locatelli et al., 2014; Stovin et al., 2013) ,
164 and numerical models by using commercial software such as HYDRUS (Hakimdavar et
165 al., 2014; Hilten et al., 2008; Palla et al., 2012), EPA’s SWMM (Bonoli et al., 2013;
166 Burszta-Adamiak and Mrowiec, 2013; Krebs et al., 2014; Palla and Gnecco, 2015;
167 Versini et al., 2015), MIKE URBAN (Locatelli et al., 2014), SWMS-2D and SWAP (see
168 Li and Babcock, (2014) and Elliott and Trowsdale (2007) for an overview). Among
169 several models used in GR studies, the gaps in model capabilities, in particular in long-
170 term simulation, are continuously narrowed.

171 Li and Babcock (2014) underline that SWMM is a quick and valid assessment tool for
172 quantifying the hydrological performance of a GR, which is also confirmed by the study
173 of Palla and Gnecco (2015), who found that the LID (Low Impact Development) modules
174 of SWMM, if correctly calibrated and validated (on an event basis, using events generated
175 under controlled conditions in the laboratory), can be successfully implemented to study
176 the hydrological response of a small urban catchment. On the contrary, Burszta-Adamiak

177 and Mrowiec (2013) observed that SWMM has limited capabilities in correctly
178 simulating the hydrograph of storm water runoff from a GR. However, simulations in
179 both studies were conducted for each analyzed event separately (single event
180 simulations), without taking into account the evapotranspiration (ET) process and the
181 restoration of retention capacity associated with it. On the contrary, as highlighted by
182 many authors (Berretta et al., 2014; Locatelli et al., 2014; Marasco et al., 2014; Poë et al.,
183 2015; Stovin et al., 2012; Yang et al., 2014) ET is a keystone in long-term simulations,
184 because it is the hydrological process responsible for the movement of water to the air
185 from sources such as the substrate, the vegetation, and the drainage layer. Therefore, ET
186 restores the GR's water holding capacity increasing its retention capacity. In this
187 framework the present manuscript will provide a long-term simulation model that takes
188 into account the evaporation process as well.

189 **1.3 Objectives**

190 The first objective of this study is to present the hydrological monitoring results of a full-
191 scale extensive commercial GR located in Bologna (Italy), with the intent of filling a gap
192 in knowledge of the stormwater retention performance of a full-scale commercial green
193 roof in a temperate sub-continental climate region.

194 The second goal of the study is to simulate the hydrological performance of GRs by
195 means of SWMM using the LID control modules (version 5.1.010) using long-term
196 rainfall and temperature data. For this purpose, a commercial extensive GR has been
197 modelled using the “bio-retention cell” LID module and the model has been calibrated
198 and validated based on the measurement results obtained from rainfall and runoff
199 monitoring presented in the first part of the study.

200 **2 METHODOLOGY**

201 **2.1 Site description**

202 A full-scale GR and an adjacent impervious roof area, both located above the LAGIRN
203 laboratory (44.513058°N, 11.318787°E) at the Engineering Campus of the University of
204 Bologna (UNIBO) have been used as case study.

205 The city of Bologna is located in northern Italy and has a humid temperate subcontinental
206 climate with hot and muggy summers, cold winters, no dry season (Toreti et al., 2010)
207 and an average precipitation of 700-800mm/year (Brunetti et al., 2006).

208 The experimental site (Bonoli et al., 2013; Maglionico et al., 2014) occupies about 120
209 m² of an existing flat roof, which was divided in two areas: one devoted to a newly added
210 extensive commercial GR (Sedum Roof, SR), while the other area was retrofitted with a
211 new membrane and was left bare as control plot (Reference Roof, RR) (Fig. 1). The SR
212 (5.15 m x 11.30 m), with a slope of 0.5 %, is a built-in-place system realized using a
213 commercial "green roof package" provided by Harpo Spa, Trieste, Italy, fully described
214 in other studies (Palla and Gnecco, 2015; Raimondo et al., 2015; Savi et al., 2013) (Fig.
215 1). Six layers were laid in sequence above the flat concrete roof, from bottom to top: a) 4
216 mm of waterproofing PVC root barrier membrane; b) 3 mm of protection fabric; c) 25
217 mm of drainage; d) 0.5 mm of filter fabric; e) 100 mm of substrate to support plant
218 growth; and f) a mix of Sedum vegetation (Fig. 1).

219 The GR plot is surrounded by a gravel strip (10 cm deep and 30 cm wide), placed above
220 the layers (a-d), previously described, in place of the substrate (Fig. 1). The RR (5.15 m
221 x 11.30 m), consists of a concrete flat roof insulated using a waterproofing PVC
222 membrane (Fig. 1).



223

224

225

226

Fig. 1. Aerial view of the experimental site showing: the extensive green roof (SR) and the reference roof (RR), the position of the in-pipe flow meters (W15 and W14 respectively for RR and SR), the position of the weather station and the stratigraphy of the green roof.

227

2.2 Experimental setup and instrumentation

228

229

230

231

232

233

234

235

236

237

238

239

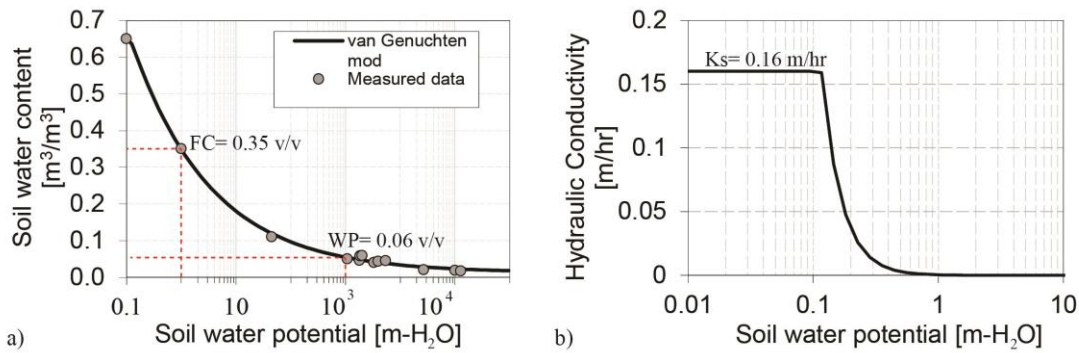
Each plot (SR and RR) has its own single, internal downspout (Fig. 1) and water cannot migrate from one plot to the other. Runoff from both plots was measured using two in-pipe flow meters, W14 and W15 for the SR and RR respectively (Fig. 1), designed at Columbia University (NYC) as those used in other studies (Carson et al., 2013; Hakimdavar et al., 2014) and directly connected to a HOBO Onset weather station. The aforementioned flow meters consist of a runoff chamber with an outlet weir and a Senix TSPC-30S1 ultrasonic sensor. The ultrasonic sensor detects the rise in water height and adjusts its output voltage accordingly. The voltage reading can then be related to a water flow rate by a calibration equation, to determine the runoff depth. The flow meters, the operating procedure and data transmission to the HOBO logger system is fully described in the study written by Carson et al. (2013). The Onset HOBO U30 weather station installed on site, above the GR plot, as showed in Fig. 1, records: rainfall, wind speed,

240 gust speed, wind direction, relative humidity, atmospheric temperature, dew point, solar
241 radiation and photosynthetically active radiation (PAR) at 5-minute intervals. Since May
242 2014, a Decagon's ECH2O sensor directly connected to the weather station, has
243 monitored the volumetric water content of the soil by measuring the dielectric constant
244 of the soil, which is a strong function of water content. Together with the sensor's data,
245 this information is sent to a Wi-Fi data logger and an online platform, from which they
246 can be easily accessed.

247 Single runoff events were defined following the procedure illustrated by other studies
248 (Carson et al., 2013; Hakimdavar et al., 2014; Nawaz et al., 2015; Vanwoert et al., 2005):
249 a storm event begins when rainfall is first recorded, with a minimum rain gauge sensitivity
250 of 0.2 mm, and ends when no precipitation or runoff has been recorded for 6 hours.
251 Afterwards, storm events were considered unsuitable for analysis and were discarded if
252 they followed any of these unacceptability conditions: 1) the recorded peak runoff rate
253 caused the depth of water behind the weir device face to exceed 90% of the notch height
254 (in fact when flow rates exceed this amount, the turbulence within the runoff chamber
255 could cause unreliable readings); 2) precipitation was in the form of snow; 3) the
256 cumulative runoff exceeded total rainfall, and 4) the ultrasonic sensor lost power over the
257 course of the storm event (see Carson et al. (2013) for more details).

258 Laboratory tests were performed to measure the physical properties and the water
259 retention characteristics of the substrate. Tests included: particle size distribution, bulk
260 density, particle density, porosity, water retention and hydraulic conductivity. Moisture
261 release curves were determined using a WP4-T dew point meter (Decagon Devices,
262 Pullman, WA) following the procedure illustrated by Bittelli and Flury (2009). To
263 determine soil water fluxes in unsaturated soils, a common approach is to numerically

264 solve the Richards equation, which generally requires the parametrization of the soil
 265 water retention curve (Bittelli and Flury, 2009; Campbell, 1985). The physical
 266 characteristics of the substrate and the parameters, obtained from the fitting with the
 267 modified van Genuchten-Mualem model (Ippisch et al., 2006) of the water retention
 268 curve, are listed in Table 2, and the corresponding curves are shown in Fig. 2.
 269 Fig. 2a shows the soil water retention curve, used to determine the Field Capacity (FC) at
 270 0.01 bar suction and the permanent Wilting Point (WP) at 15 bar suction (as provided by
 271 the Italian standard (UNI EN 13041, 2012); while Fig. 2b shows the hydraulic
 272 conductivity curve used to obtain the saturated hydraulic conductivity (Ks).



273 a) b)
 274 **Fig. 2.** Soil water retention curve (a) and hydraulic conductivity (b) for the 10 cm deep substrate (FC,
 275 field capacity at 0.01 bar suction; WP, wilting point at 15 bar suction; and Ks, saturated hydraulic
 276 conductivity).

277

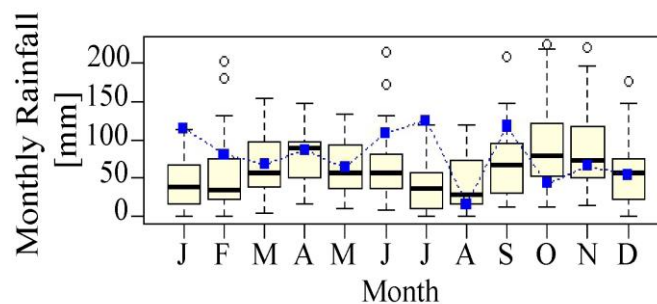
Parameter	System Unit	Substrate
D ₅₀	mm	6
Particle density, ρ_p	g/cm ³	2.70
Dry density, ρ_{dry}	g/cm ³	0.90
Porosity, n	%	62 %
Field capacity	m ³ /m ³	0.35
Wilting point	m ³ /m ³	0.06
Organic content	%	<4

278

Table 2. Substrate characteristics.

279 **2.3 Climate analysis**

280 The average rainfall in the city of Bologna fluctuates from around 400 mm to 1,000 mm
281 a year. Most of the rainfall events usually occur in spring and fall. Although snow events
282 are not uncommon, there was no snow during this case study monitoring period.



283

284 **Fig. 3.** Boxplot of the historical rainfall recorded over 26 years (1990-2015) for the city of Bologna. The
285 bottom and the top of the box are the first and third quartiles, and the band inside the box is the second
286 quartile (the median). The ends of the whiskers represent the lowest and the highest datum. Any data not
287 included between the whiskers have been plotted as outliers. The blue trend line (square indicators)
288 indicates the case study monthly rainfall depths for the monitoring period (from Jan/2014 to Dec/2014).

289 The climatic conditions gathered from the case study HOBO weather station over 12
290 months (January 2014 – December 2014) were compared to the historical data provided
291 by the Regional Agency for Prevention, Environment and Energy in the Emilia-Romagna
292 region, Italy (ARPAE, 2016). The variation of monthly rainfall, over 26 years (1990-
293 2015), is shown in Fig.3 through the use of a box-plot for each month of the year, while
294 the blue trend line (square indicators) shows the total monthly rainfall during the
295 monitoring period. Overall, the rainfall data during the study period are consistent with

296 the historical rainfall data. The cumulated monthly rainfall is above its average historical
297 value for eight months out of 12, in particular summer 2014 was very rainy. During the
298 months of June, July and September the rainfall was far above the median, while in
299 August it was slightly below the median of the historical data.

300 **3 EPA SWMM MODEL**

301 **3.1 Presentation of EPA SWMM**

302 The EPA Storm Water Management Model (SWMM, version 5.1.010) was selected as
303 the modelling platform for studying the hydrologic response of both the green roof and
304 the conventional plot. SWMM is a dynamic hydrology-hydraulic and water quality
305 simulation model that was primarily developed for urban areas allowing short and long-
306 term simulations (Rossman, 2015, 2010).

307 LID control modules that provide detention storage, enhanced infiltration and
308 evapotranspiration of runoff from localized surrounding areas (e.g. rain garden, bio-
309 retention cell, permeable pavement, infiltration trench, etc.) have been implemented in
310 SWMM to simulate the hydrological behaviour of such source control technologies since
311 2005 (Palla and Gnecco, 2015; Rossman, 2015; Versini et al., 2015). LID controls are
312 represented by a combination of vertical layers whose properties (such as: thickness of
313 the different layers, physical properties of the materials, and underdrain characteristics)
314 are defined on a per-unit-area basis (Qin et al., 2013). This allows LIDs which differ in
315 areal coverage only, and not in design, to be easily placed within different subcatchments
316 in a study area (Palla and Gnecco, 2015).

317 To take into account the impact of climate data on the LID retention performance and
318 compute the potential daily evapotranspiration, SWMM offers a climatology editor

319 function with a single set of time-dependent temperatures applied throughout the study
320 area (Rossman, 2015). Maximum and minimum daily temperatures and the study area's
321 latitude are used by the software to compute the potential evapotranspiration applying the
322 Hargreaves method (Hargreaves and Samani, 1985), fully illustrated by Rossman (2016,
323 2015).

324 **3.2 Modelling the green roof plot using the SWMM LID modules**

325 Starting from version 5.1 (2014), the SWMM software is equipped with an additional
326 LID module for GR modelling, "Green Roof" LID Type (GR-LID), which is a variation
327 of a "Bio-Retention Cell" LID Type (BRC-LID). Generally, LID Controls are defined
328 and assigned to subcatchments through a series of three different editor forms: i) The LID
329 Control Editor, ii) the LID Group Editor and, iii) LID Usage Editor.

330 The LID Control editor is used to define a low impact development control that can be
331 deployed throughout a study area to store, infiltrate, and evaporate subcatchment runoff
332 (such as: bio-retention cell, rain garden, green roof, infiltration trench, permeable
333 pavement, rain barrel, or vegetative swale). The LID Group Editor is used to add any type
334 of LID controls to a specific subcatchment. Finally, the LID Usage Editor is used to
335 describe how each LID control added to a LID group is deployed within the group's
336 subcatchment. It is nested under the LID Group Editor to be able to specify the areal
337 extent of the control, the portion of the subcatchment's runoff that it treats, and for some
338 LID the "% Initially saturated" which define the degree to which the unit's soil is initially
339 filled with water.

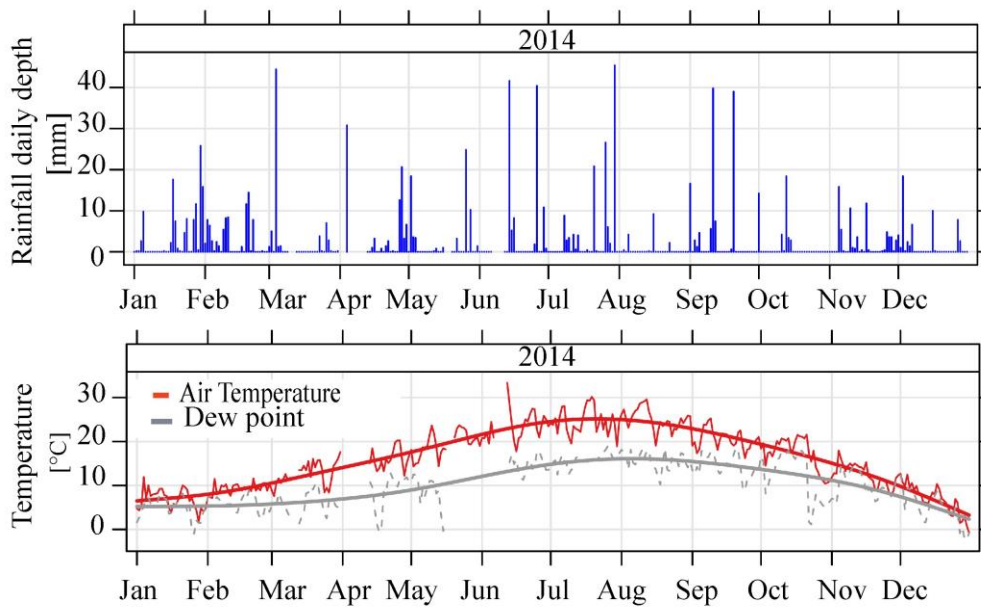
340 A GR-LID is composed of three layers: surface (vegetation), soil (substrate), and drainage
341 material, while the BRC-LID differs because of the presence of two layers (storage and

342 drain) instead of the drainage material only. The main difference between these LID types
343 is that in the GR-LID the drain system is design-based, while in the BRC-LID it is
344 performance-based (Rossman, 2016).

345 Palla and Gnecco (2015) demonstrate that a GR-LID can be successfully used for
346 modelling the hydrological behavior of a GR, by using the property of the soil as
347 calibration parameters and by fixing, as initial condition, the soil moisture content of the
348 LID before each simulated event (“% Initially saturated” parameter). However, when the
349 geometry of the drainage material is not standard, when all the physical properties of the
350 layers are measured in laboratory, and last but not least when the degree of saturation of
351 the LID before each storm event is automatically calculated by the model, as in a long-
352 term simulation, the only way to regulate the outflow is the calibration of two parameters
353 of the drain layer of a BRC-LID called "Drain coefficient" and "Drain exponent".
354 Through these two parameters the software determines the flow rate through the drain
355 itself (Rossman and Huber, 2016).

356 Based on the above considerations, in the present study the full-scale GR has been
357 modelled by coupling two LID modules: i) a bio-retention cell for the GR system, and ii)
358 a porous pavement for the gravel strip, both LID modules fully occupy the respective
359 subcatchment.

360 As recommended by several authors (Alfredo et al., 2010; Burszta-Adamiak and
361 Mrowiec, 2013; Mrowiec et al., 2014; Zhang and Guo, 2014), the SWMM LID model
362 (SR surface) and the SWMM model (RR surface) have been calibrated and validated
363 based on the experimental monitoring data.



364

365

Fig. 4. Data acquisition during year 2014: cumulative daily rainfall (mm) (top), average hourly air

366

temperature (°C) and dew point (°C) (bottom).

367

3.3 Input data

368

The rainfall and air temperature recorded by the on-site HOBO weather station in 2014,

369

were used as input data to calibrate and validate the model. Fig. 4 shows the daily

370

distribution of rainfall and the hourly average air temperature over year 2014.

371

In order to simulate the evapotranspiration process in a GR which is responsible for

372

decreasing the substrate moisture content and thus for restoring the retention capacity of

373

a GR (Berretta et al., 2014), the climatology editor of SWMM was set up. The software

374

automatically applies an empirical formula (Hargreaves and Samani, 1985) for estimating

375

potential daily evapotranspiration (ET_0) that depends on daily air temperature and solar

376

radiation at the study site. However, potential evapotranspiration (ET_0) differs from real

377

evapotranspiration (ET_r) because the first is related to a reference crop, which can be

378

either grass or alfalfa (Hargreaves et al., 1985), and is affected only by climatic

379 parameters, while the second is influenced by the type of plants, crop characteristics and
 380 cultivation practices (Allen et al., 1998). In the case of GRs, the real evapotranspiration
 381 may deviate from ET_0 due to the use of a non-standard plant (sedum) and of non-optimal
 382 conditions, such as low soil fertility, water shortage or waterlogging. To take into account
 383 this, in the present study the Hargreaves equation was adapted to the SR case specifying
 384 a monthly soil recovery pattern (Table 3), whose factors, multiplied by ET_0 , transform
 385 ET_0 in ET_r and then adjust the rate at which infiltration capacity is recovered during
 386 periods with no precipitation.

Month	Value
January	0.05
February	0.05
March	0.15
April	0.60
May	1.00
June	1.15
July	1.15
August	1.15
September	0.30
October	0.20
November	0.15
December	0.05

387 **Table 3:** Monthly soil recovery pattern.

388 These coefficients were found through a procedure which takes into consideration, in
 389 similitude with the study done by Berretta et al. (2014), the experimental measurements
 390 of the substrate moisture content during dry periods and the comparison with simulated
 391 moisture content using a hydrologic model based on water balance and on the Hargreaves
 392 ET_0 model. Altogether, these coefficients incorporate mainly crop characteristics and
 393 averaged effects of evaporation from the soil over the length of the growing season
 394 (Cipolla, 2015).

395 **3.4 Calibration and validation procedures**

396 Model calibration and validation is based on the comparison of the observed and modeled
397 runoff flow rates. In order to assess the model performance on an event basis, the RMSE-
398 Observation Standard Deviation Ratio (RSR) was calculated. The RSR is the ratio of the
399 root mean square error (RMSE) to the standard deviation of measured data, and varies
400 from the optimal value of 0, to a large positive value (Moriasi et al., 2007). Lower values
401 of RSR correspond to lower RMSE values and to a better model simulation performance.
402 Furthermore, the Nash–Sutcliffe Efficiency index (NSE) was evaluated to quantitatively
403 assess the model accuracy in reproducing the runoff flow rate on an event basis (Nash
404 and Sutcliffe, 1970).

405 **4 RESULTS AND DISCUSSION**

406 **4.1 Hydrological Experimental Observations**

407 Rainfall and runoff were continuously collected from 01/01/2014 to 31/12/2014 for the
408 SR plot, whereas only from 01/01/2014 to 31/05/2014 for the RR.

409 The monitoring campaign resulted in 69 and 23 valid runoff measurements, from the
410 original 122 storm events recorded, respectively for the SR and RR. Unfortunately, after
411 3 months of data collection, the W15 flow meter had a malfunction which temporary
412 interrupted the recording of runoff data, thus a statistical analysis of those data will not
413 be presented.

414 The measured rainfall depth of the 69 storm events, that generated a valid runoff
415 measurement for SR, ranged from 0.2 to 41.6 mm, while the normalised runoff varied
416 from 0 to 33.1 mm. Rainfall attenuation of individual events ranged widely from 6.4% to

417 100%. The total number of storm events that generated zero runoff was 34 out of which
418 19 had a rainfall depth higher than 0.2 mm; the largest event with 100% retention was 7.8
419 mm (26/03/2014). During the monitoring period the SR has demonstrated a retention
420 capacity of 51.9% of the total rainfall volume from suitable events. This may be compared
421 to the previously-published annual retention data for similar GRs (Table 1). From a range
422 of studies, including only full-scale installation with 10 cm of substrate depth, the
423 retention capacity ranged between 12% and 74% (Berkompas et al., 2008; Carson et al.,
424 2013; Hutchinson et al., 2003; Liu and Minor, 2005; Moran et al., 2005; Spolek, 2008).
425 The performance of the Bologna full-scale GR falls slightly above the average value
426 (46.7%) of previously reported data (Table 1).

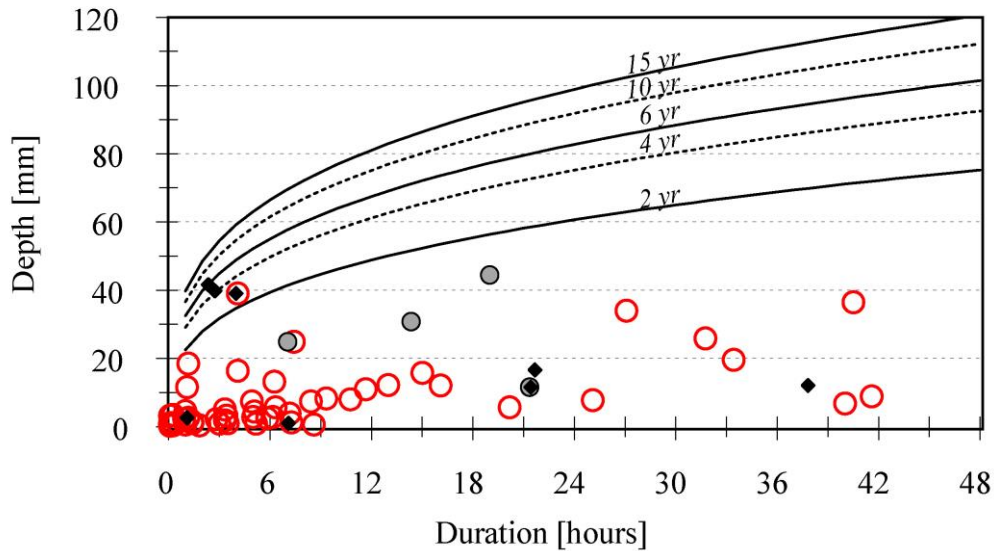
427 **4.2 Calibration and validation results**

428 The experimental site was simplified in 3 subcatchments: two for simulating the SR plot
429 and one for the RR, 4 junctions, 2 outfalls, and 4 conduits.

430 The model was calibrated over 6 events (2 for the RR and 4 for the SR), reported in Table
431 4, and was verified by simulating a complete 1 year (2014) data period and then validated
432 with 6 rain events (2 for the RR and 4 for the SR) spread out along the year.

433 The experimental rainfall time series were analyzed against Bologna historical records
434 obtained from the Regional Agency for Prevention, Environment and Energy in the
435 Emilia-Romagna region, Italy (ARPAE, 2016). Fig. 5 compares all the 69 monitored
436 events (SR plot) in terms of total rainfall depth and duration (red hollow circles) to the
437 relevant Intensity-Duration-Frequency (IDF) curves taking into account the event return
438 periods found using the historical data. The majority of the events fall below the 2 year
439 return period threshold, as happened in other similar studies (Stovin et al., 2012), with 4

440 events with a return period bigger than 2 years. The rainfall record contains a reasonable
 441 distribution of short and long-duration events. The black and grey indicators in Fig. 5,
 442 show the events used for calibration and validation for the SR and RR model respectively.



443
 444 **Fig. 5.** Rainfall characteristics for the 12 month data series compared with the IDF return period curves
 445 estimated for Bologna. The black and grey full indicators show the events used for calibration and
 446 validation for the SR and RR model respectively.

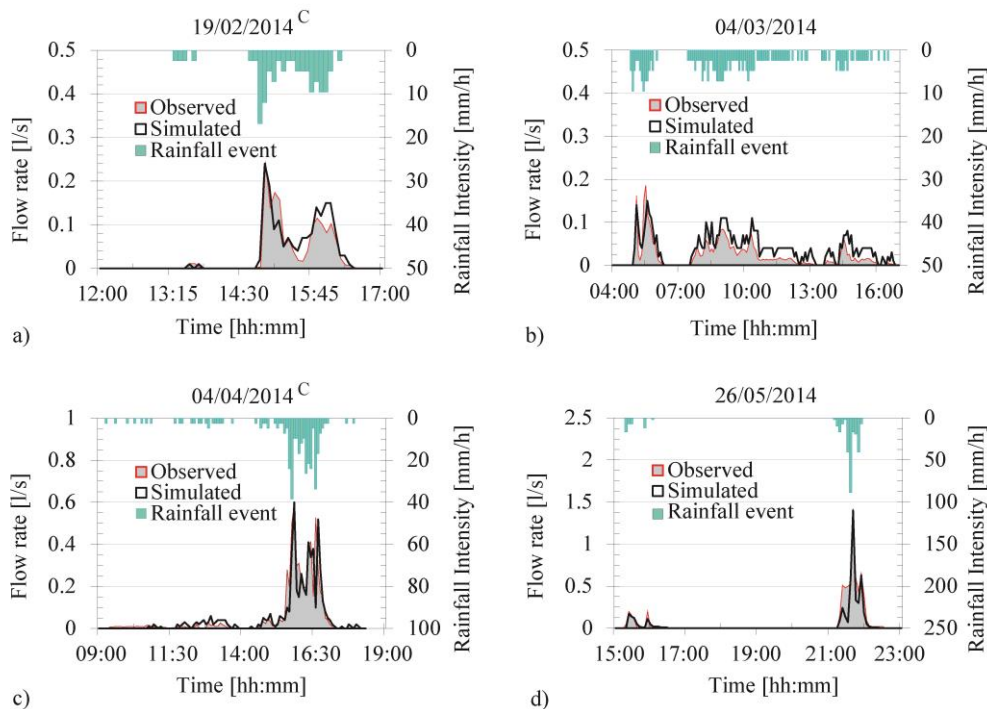
447 For the events chosen for calibration and validation the rainfall characteristics are
 448 summarized in table 4 in terms of rain duration, rainfall depth, peak intensity and return
 449 period.

450 The 12 storms vary widely (Table 4), ranging in duration from 65 minutes to almost 37
 451 hours and in depth from 2.6 to 44.4 mm. Pursuing the purpose of observing the behaviour
 452 of the model under different weather conditions, the calibration/validation events have
 453 been chosen in different seasons of the year and with a wide range of rainfall intensity
 454 and return period.

455

Plot	Events Date [dd/mm/yy]	Rain Duration [min]	Rainfall depth [mm]	Peak 5-min Intensity [mm/h]	Return period (year)					
					Event	0.5 h	1 h	3 h	6 h	12 h
RR	19/02/14 ^C	1282	11.6	16.8	<2	<2	<2	<2	<2	<2
	04/03/14	1140	44.4	9.6	<2	<2	<2	<2	<2	<2
	04/04/14 ^C	860	30.8	38.4	<2	<2	<2	<2	<2	<2
	26/05/14	440	24.8	88.8	<2	<2	<2	<2	<2	<2
SR	10-12/02/14 ^C	1300	16.6	9.6	<2	<2	<2	<2	<2	<2
	22/04/14	65	2.6	12.0	<2	<2	<2	<2	<2	
	14/06/14 ^C	140	41.6	168.0	6	48	14	5		
	11/09/14	165	39.8	48.0	4	<2	4	4.5		
	20/09/14 ^C	240	39	69.6	4	3	3	4	2	
	10-11/11/14	1285	11.6	9.6	<2	<2	<2	<2	<2	<2
	17-18/11/14 ^C	2270	12	4.8	<2	<2	<2	<2	<2	<2
	03/12/14	425	1	2.4	<2	<2	<2	<2	<2	

456 **Table 4.** Rainfall characteristics for the calibration/validation rainfall events. The superscript ‘C’ denotes
457 the calibration events.



458 **Fig. 6.** Rainfall hyetographs and the corresponding measured runoff (grey area) compared to the
459 simulated runoff (black line) for RR during 2 events used for calibration and 2 validation events. The
460

461 events correspond to: a) February 19th, 2014, b) March 4th, 2014 c) April 4th, 2014 d) May 26th, 2014. The
462 superscript ‘C’ denotes the calibration events.

463 4.2.1 The RR surface model

464 The RR model is calibrated and validated based on 4 events, measured by the on-site W15
465 flow meter and collected between February and May 2014; the February 19th, 2014 and
466 the April 4th, 2014 events were selected for the calibration phase. The rainfall intensity,
467 the observed and the modeled flow rates for the selected calibration and validation events
468 are shown in Fig. 6. While the calibrated SWMM parameters (Depression depth, N
469 Manning and % Zero-Imperv) are reported in Table 5.

SWMM Parameter	SU	Values
Depression depth	mm	1
N Manning	-	0.011
% Zero-Imperv	%	5

470 **Table 5.** Parameters assigned in the SWMM RR model.

471 Fig. 6a and Fig. 6c show the rainfall hyetograph and the corresponding simulated and
472 observed runoff for the two calibration events. The model reproduces with good matching
473 capabilities the complex-shape (multi-peaks) outflow regime for both low (< 20 mm/h)
474 and average (< 40 mm/h) rainfall intensities. The model is able to accurately reproduce
475 the timing and the magnitude of the peak flow rate. NSE values (see Table 6) are greater
476 than 0.7 confirming the suitability of the model to describe the hydrologic response of a
477 traditional impervious roof, while the low value of RSR (0.36) indicates a good model
478 performance. Fig. 6b and Fig 6d show the rainfall hyetograph and the corresponding
479 simulated and observed runoff for the validation events. The model provides a good
480 description of the runoff response (Fig.6b and Fig. 6d) both in terms of shape and peak
481 of the outflow hydrograph. NSE and RSR values (see Table 6) are good for the
482 26/05/2014 event while the performance of the model decrease for the 04/03/2014.

Plot	Events Date (dd/mm/yy)	NSE (-)	RSR (-)
<i>RR</i>	19/02/14 ^C	0.87	0.36
	04/03/14	0.41	0.77
	04/04/14 ^C	0.72	0.36
	26/05/14	0.85	0.35
<i>SR</i>	10-12/02/14 ^C	0.58	0.65
	22/04/14	0.60	0.63
	14/06/14 ^C	0.66	0.59
	11/09/14	0.85	0.39
	20/09/14 ^C	0.93	0.27
	10-11/11/14	0.44	0.75
	17-18/11/14 ^C	0.61	0.62
	03/12/14	0.76	0.49

483 **Table 6:** Nash–Sutcliffe Efficiency (NSE) index and Observation Standard Deviation ratio (RSR) of the
484 total effluent volume for the observed rainfall events used for the calibration and validation. The
485 superscript ‘C’ denotes the calibration events.

486 **4.2.2 The SR green roof model**

487 The SR numerical model is developed by coupling two LID modules, as explained in
488 section 3.2. The model is calibrated based on experimental rainfall/runoff data collected
489 in 2014 for the full-scale SR. Table 7 shows the parameters required by the bio-retention
490 cell and the permeable pavement LID control modules. The SR model is calibrated and
491 validated based on 8 events measured by the W14 flow meter and collected between
492 February and December 2014 (Table 4 and Table 6).

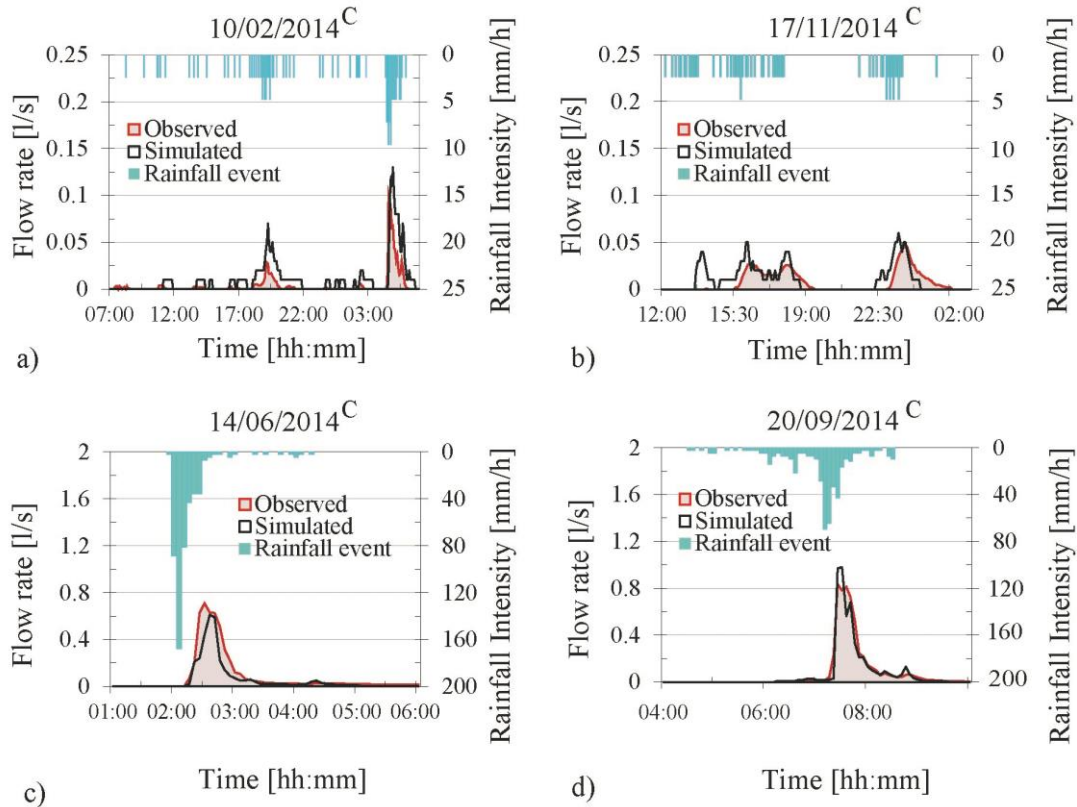
493 Burszta-Adamiak and Mrowiec (2013) affirm that the main parameter influencing the
494 simulation results of a LID is called "% Initially saturated" (specified in LID Usage
495 Editor). For each LID type this parameter expresses the degree to which the unit's
496 substrate is initially filled with water (0% saturation corresponds to the wilting-point
497 moisture content, 100% saturation has the moisture content equal to the porosity). Also
498 Palla and Gnecco (2015) recognize the importance of this parameter by doing a sensitivity
499 analysis to understand how the uncertainty in the outflow (such as volume, peak and

500 shape) can be apportioned to different sources of uncertainty compared to the initial
501 moisture content value. Pursuing the goal of reducing the dependence of the model on
502 this parameter, its value was set equal to 100%, as initial condition. This means that it is
503 the model itself that, as a function of the weather data and of the ET rate, estimates the
504 degree of saturation of LIDs before a rainfall event. This assumption generates a runoff
505 rate during the first day (01/01/2014) of the long-term simulation, which disappears from
506 the second day forward. Furthermore, during the second day of simulation (02/01/2014)
507 the substrate moisture content in the model has a value equal to the field capacity (0.35
508 v/v), which is coherent with the results of on field moisture content measurements made
509 in January 2014 and 2015 by the authors.

Layer	Parameter	SU	Bio- retention Cells	Permeabl e Pavement
Surface	Berm Height	mm	3	3
	Vegetation Volume Fraction		0.15	0
	Surface Roughness	m ^{1/3} /s	0.2	0.02
	Surface Slope	%	0.5	0.5
	Pavement	Thickness	mm	-
Void Ratio			-	0.4
Impervious Surface Fraction			-	0
Permeability		mm/h	-	3000
Clogging Factor			-	0
Soil	Thickness	mm	100	-
	Porosity	%	0.65	-
	Field Capacity	m ³ / m ³	0.35	-
	Wilting Point	m ³ / m ³	0.06	-
	Conductivity	mm/h	160	-
	Conductivity Slope		5	-
	Suction Head	mm	25	-
Storage	Thickness	mm	25	25
	Void Ratio		0.5	0.5
	Seepage Rate	mm/h	0	0
	Clogging Factor		0	0

Underdrain	Drain Coefficient	2	0.15
	Drain Exponent	2.1	1.6
	Offset Height	mm 3	3

510 **Table 7:** Parameters assigned in the SWMM model-LID control section for the GR (modelled as a bio-
511 retention cell) and for the gravel stripe (modelled as a permeable pavement).



512
513 **Fig. 7:** The rainfall hyetographs and the corresponding measured runoff (grey area) compared to the
514 simulated runoff (black line) for SR during 4 events used for calibration. The events correspond to: a)
515 February 10th, 2014; b) November 17th, 2014; c) June 14th, 2014 and d) September 20th, 2014.

516 The hyetographs, the corresponding measured and simulated hydrographs for the four
517 calibration events are illustrated in Fig. 7, while the NSE and the RSR index for both
518 calibration and validation events are reported in Table 6. During the calibration phase the
519 SR model showed a good ability in reproducing the complex-shape outflow, in particular
520 the magnitude and the timing of the peak flow rate were accurately predicted in all the
521 seasons (Fig. 7), as confirmed by NSE values >0.58 and RSR <0.65 . Results of the

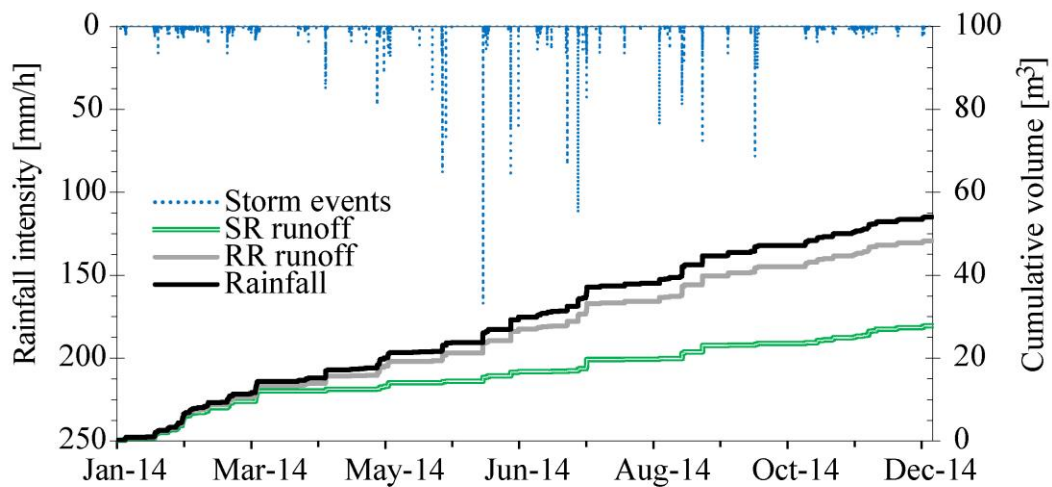
522 validation procedure confirm the suitability of the model in reproducing the outflow: not
523 only the mean NSE value is 0.66 (standard deviation 0.032) for the four validation events,
524 but also the average RSR is 0.56 (standard deviation 0.025); those values clearly reveal
525 the model accuracy in predicting the outflow of the full-scale GR.

526 **4.3 Long term simulation in SWMM**

527 Once the RR and SR models were calibrated and validated on experimental measurements
528 of rainfall and relative runoff, a one-year simulation was launched. Summarizing from
529 above, the input data were: the rainfall data with a 5-minute time step, the maximum and
530 minimum daily temperatures, the latitude of the site, and a set of monthly soil recovering
531 coefficients (Table 3). In addition, the LID modules were considered fully saturated, as
532 initial condition.

533 Predicted cumulative runoff at the SR plot is in good agreement with the experimental
534 measurements. The cumulative outflow volume of the 69 measured events, was in fact
535 only 9% lower than the discharge volume obtained through the SWMM modeling, which
536 proves the ability of the model in predicting the overall hydrological process. Fig. 8 shows
537 that in winter (Jan-Mar 2014), the difference between the runoff from RR and SR is
538 minimal. This is certainly due to the fact that the substrate moisture content never drops
539 below the field capacity. The cumulative annual water balance is displayed in Fig. 8 for
540 the SR and RR plots respectively. The simulated cumulative runoff volumes were 48.1
541 m³ and 27.7 m³, respectively for RR and SR, and correspond to an annual retention of
542 11% and 48%. The cumulative retention results demonstrate that the SR, despite having
543 only 10 cm of substrate depth, can make a significant contribution in reducing the total
544 volume of stormwater that might otherwise impact watercourses, require treatment or

545 flood the city.



546

547 **Fig. 8.** Storm events (blue line), cumulative rainfall (black line) and cumulative simulated runoff from the
548 conventional RR (gray line) and the green roof SR (green line).

549 **5 CONCLUSION**

550 GRs are becoming one of the key technologies for achieving a sustainable urban drainage
551 system; however, their level of performance is very site specific because of the impact of
552 the layer materials, vegetation, physical properties of the substrate, design specification
553 and climate conditions. Furthermore, the hydrological performance of a GR is strongly
554 influenced by the size of the studied plots (full-scale vs small scale), the definition of
555 "event", and the number of events included in the study (Carson et al., 2013).

556 Experimental studies have the ability to narrow the gap between hydrological model
557 simulations and reality, especially if performed on full-scale green roofs with the support
558 of field data monitoring.

559 Given the above, this study first provided an accurate review of the scientific literature,
560 with a focus on experimental studies on full-scale installation. Previous studies found that
561 the annual retention volume can range from 11.0 % to 76.4 % with an average retention

562 value of 46.7% (Table 1). In addition, the study provided a synthetic literature review
563 about hydrological models in this field, which also underlined the difficulty of complete
564 numerical models in long terms simulations.

565 The second part of the study was devoted to the description of the experimental site and
566 instrumentation. The results of the monitoring campaign performed from January 2014
567 to December 2014 were later used to calculate the experimental green roof's (SR) annual
568 average retention, found to be 51.9 %. This value falls in the average range of the values
569 indicated by previous studies (Table 1).

570 Finally, the study described a numerical model realized by means of SWMM 5.1, which
571 was calibrated and validated using field measurements and then used to simulate the long
572 term hydrologic response of two adjacent experimental surfaces of the same size: an
573 impervious and a green full-scale roof. Modelling results confirmed the role of GRs in
574 restoring the natural regime reducing the annual runoff volume. The comparison of the
575 results obtained for the experimental green roof SR to the SWMM simulation results
576 proved that the suggested model has good capabilities in correctly simulating the
577 hydrograph of storm water runoff from GRs along the year. This is confirmed by the quite
578 high values of NSE and the low values of RSR obtained in both the calibration and
579 validation phases. Furthermore, the low difference (< 9%) in total retention between the
580 69 measured and simulated events confirms the suitability of the model for long-term
581 simulations.

582 The proposed modelling approach demonstrated that SWMM can be suitably used for
583 assessing the continuous LID performance, and consequently for supporting local
584 authorities or designers in the evaluation of the hydrological efficiency of green roofs.

585 **ACKNOWLEDGEMENTS**

586 The authors would like to acknowledge the CIRI EC (Interdepartmental Center for
587 Industrial Research, Building and Construction), DICAM (Department of Civil,
588 Chemical, Environmental and Materials Engineering) and AUTC (UNIBO Facility
589 Management Office) of the University of Bologna (Italy) for funding the experimental
590 site and instrumentation. Thanks to Prof. A. Bonoli and Dr. A. Conte (DICAM) for their
591 pivotal role in creating and developing the Bologna experimental green roofs project, and
592 to Prof. M. Speranza and Dr. L. Ferroni, from the Department of Agricultural Sciences,
593 for their assistance with the project, for helping in the study of the vegetation and for
594 providing the physical properties of the substrate. Special thanks also to Prof. P. J.
595 Culligan “green infrastructures group” of Columbia University (NYC) and especially to
596 Dr. T. B. Carson and Dr. D. E. Marasco for providing the runoff sensors and assistance
597 with data monitoring.

598 **REFERENCE**

- 599 Alfredo, K., Montalto, F., Goldstein, A., 2010. Observed and Modeled Performances of
600 Prototype Green Roof Test Plots Subjected to Simulated Low- and High-Intensity
601 Precipitations in a Laboratory Experiment. *J. Hydrol. Eng.* 15, 444–457.
602 doi:10.1061/(ASCE)HE.1943-5584.0000135
- 603 Allen, R.G., Pereira, L.S., Raes, D., Smith, M., 1998. Crop evapotranspiration:
604 Guidelines for computing crop requirements. *Irrig. Drain. Pap. No. 56*, FAO 300.
605 doi:10.1016/j.eja.2010.12.001
- 606 ARPAE, 2016. http://www.arpae.it/dettaglio_generale.asp?id=3284&idlivello=1625
- 607 Beecham, S., Razzaghmanesh, M., 2015. Water quality and quantity investigation of

608 green roofs in a dry climate. *Water Res.* 70, 370–384.
609 doi:10.1016/j.watres.2014.12.015

610 Bengtsson, L., Grahn, L., Olsson, J., 2005. Hydrological function of a thin extensive
611 green roof in southern Sweden. *Nord. Hydrol.* 36, 259–268.

612 Berardi, U., GhaffarianHoseini, A., GhaffarianHoseini, A., 2014. State-of-the-art analysis
613 of the environmental benefits of green roofs. *Appl. Energy* 115, 411–428.
614 doi:10.1016/j.apenergy.2013.10.047

615 Berghage, R., Beattie, D., Jarrett, A., Thuring, C., Razaeei, F., O’Connor, T., 2009. Green
616 Roofs for Stormwater Runoff Control. EPA/600/R-09/026.

617 Berkompas, B., Marx, K., Wachter, H., Beyerlein, D., Spencer, B., 2008. A study of green
618 roof hydrologic performance in the cascadia region, in: 2008 International Low
619 Impact Development Conference. pp. 1–10.

620 Berretta, C., Poë, S., Stovin, V., 2014. Reprint of “Moisture content behaviour in
621 extensive green roofs during dry periods: The influence of vegetation and substrate
622 characteristics.” *J. Hydrol.* 516, 37–49. doi:10.1016/j.jhydrol.2014.04.001

623 Bertocchi, I., Fini, G., Rubolino, M.C., Tondelli, S., 2011. Sustainability achievements in
624 building regulations. the example of Bologna. *Procedia Eng.* 21, 957–967.
625 doi:10.1016/j.proeng.2011.11.2100

626 Bianchini, F., Hewage, K., 2012. Probabilistic social cost-benefit analysis for green roofs:
627 A lifecycle approach. *Build. Environ.* 58, 152–162.
628 doi:10.1016/j.buildenv.2012.07.005

629 Bittelli, M., Flury, M., 2009. Errors in Water Retention Curves Determined with Pressure
630 Plates. *Soil Sci. Soc. Am. J.* 73. doi:10.2136/sssaj2008.0082

631 Blank, L., Vasl, A., Levy, S., Grant, G., Kadas, G., Dafni, A., Blaustein, L., 2013.

632 Directions in green roof research: A bibliometric study. *Build. Environ.* 66, 23–28.
633 doi:10.1016/j.buildenv.2013.04.017

634 Bliss, D.J., Neufeld, R.D., Ries, R.J., 2009. Storm water runoff mitigation using green
635 roof. *J. Ries. Environ. Eng. Sci.* 26, 407–418. doi:doi:10.1089/ees.2007.0186

636 Bonoli, A., Conte, A., Maglionico, M., Stojkov, I., 2013. Green Roofs For Sustainable
637 Water Management. *Environ. Eng. Manag. J.* 12, 153–156.

638 Brunetti, M., Maugeri, M., Monti, F., Nanni, T., 2006. Temperature and precipitation
639 variability in Italy in the last two centuries from homogenised instrumental time
640 series. *Int. J. Climatol.* 26, 345–381. doi:10.1002/joc.1251

641 Burszta-Adamiak, E., Mrowiec, M., 2013. Modelling of Green roofs' hydrologic
642 performance using EPA's SWMM. *Water Sci. Technol.* 68, 36–42.
643 doi:10.2166/wst.2013.219

644 Campbell, G.S., 1985. *Soil Physics with Basic: Transport models for soil-plant systems.*
645 Elsevier, Amsterdam.

646 Carbone, M., Garofalo, G., Nigro, G., Piro, P., 2014. A conceptual model for predicting
647 hydraulic behaviour of a green roof. *Procedia Eng.* 70, 266–274.
648 doi:10.1016/j.proeng.2014.02.030

649 Carson, T.B., Marasco, D.E., Culligan, P.J., McGillis, W.R., 2013. Hydrological
650 performance of extensive green roofs in New York City: observations and multi-
651 year modeling of three full-scale systems. *Environ. Res. Lett.* 8, 1–13.
652 doi:10.1088/1748-9326/8/2/024036

653 Cipolla, S.S., 2015. *Tetti verdi: analisi sperimentale e simulazione numerica.* PhD
654 Thesys. University of Bologna.

655 Cipolla, S.S., Maglionico, M., Stojkov, I., 2016. Experimental Infiltration Tests on

656 Existing Permeable Pavement Surfaces. *Clean - Soil, Air, Water* 44, 89–95.
657 doi:10.1002/clen.201400550

658 Collins, K. a., Hunt, W.F., Hathaway, J.M., 2008. Hydrologic Comparison of Four Types
659 of Permeable Pavement and Standard Asphalt in Eastern North Carolina. *J. Hydrol.*
660 *Eng.* 13, 1146–1157. doi:10.1061/(ASCE)1084-0699(2008)13:12(1146)

661 Connelly, M., Liu, K., Schaub, J., 2006. BCIT Green Roof Research Program, Phase 1
662 Summary of Data Analysis: Observation Period – Jan. 1, 2005 to Dec. 31, 2005.

663 Czemieli Berndtsson, J., 2010. Green roof performance towards management of runoff
664 water quantity and quality: A review. *Ecol. Eng.* 36, 351–360.
665 doi:10.1016/j.ecoleng.2009.12.014

666 Elliott, A.H., Trowsdale, S.A., 2007. A review of models for low impact urban
667 stormwater drainage. *Environ. Model. Softw.* 22, 394–405.
668 doi:10.1016/j.envsoft.2005.12.005

669 European Commission, 2015. Call H2020-SCC-NBS-2016
670 [https://ec.europa.eu/research/participants/portal/desktop/en/opportunities/h2020/calls/h2020-scc-2016-2017.html#c,topics=callIdentifier/t/H2020-SCC-2016-2017/1/1/1/default-group&callStatus/t/Forthcoming/1/1/0/default-](https://ec.europa.eu/research/participants/portal/desktop/en/opportunities/h2020/calls/h2020-scc-2016-2017.html#c,topics=callIdentifier/t/H2020-SCC-2016-2017/1/1/1/default-group&callStatus/t/Forthcoming/1/1/0/default-group&callStatus/t/Open/1/1/0/default-)
671 [group&callStatus/t/Forthcoming/1/1/0/default-](https://ec.europa.eu/research/participants/portal/desktop/en/opportunities/h2020/calls/h2020-scc-2016-2017.html#c,topics=callIdentifier/t/H2020-SCC-2016-2017/1/1/1/default-group&callStatus/t/Forthcoming/1/1/0/default-group&callStatus/t/Open/1/1/0/default-)
672 [group&callStatus/t/Open/1/1/0/default-](https://ec.europa.eu/research/participants/portal/desktop/en/opportunities/h2020/calls/h2020-scc-2016-2017.html#c,topics=callIdentifier/t/H2020-SCC-2016-2017/1/1/1/default-group&callStatus/t/Forthcoming/1/1/0/default-group&callStatus/t/Open/1/1/0/default-) (accessed 7.11.16).

673

674 Fassman-Beck, E., Voyde, E., Simcock, R., Hong, Y.S., 2013. 4 Living roofs in 3
675 locations: Does configuration affect runoff mitigation? *J. Hydrol.* 490, 11–20.
676 doi:10.1016/j.jhydrol.2013.03.004

677 Fletcher, T.D., Shuster, W., Hunt, W.F., Ashley, R., Butler, D., Arthur, S., Trowsdale, S.,
678 Barraud, S., Semadeni-Davies, A., Bertrand-Krajewski, J.-L., Mikkelsen, P.S.,
679 Rivard, G., Uhl, M., Dagenais, D., Viklander, M., 2014. SUDS, LID, BMPs, WSUD

680 and more – The evolution and application of terminology surrounding urban
681 drainage. *Urban Water J.* 9006, 1–18. doi:10.1080/1573062X.2014.916314

682 Gambi, G., Maglionico, M., Tondelli, S., 2011. Water management in local development
683 plans: The case of the old fruit and vegetable market in Bologna. *Procedia Eng.* 21,
684 1110–1117. doi:10.1016/j.proeng.2011.11.2118

685 Gregoire, B.G., Clausen, J.C., 2011. Effect of a modular extensive green roof on
686 stormwater runoff and water quality. *Ecol. Eng.* 37, 963–969.
687 doi:10.1016/j.ecoleng.2011.02.004

688 Hakimdavar, R., Culligan, P.J., Finazzi, M., Barontini, S., Ranzi, R., 2014. Scale
689 dynamics of extensive green roofs: Quantifying the effect of drainage area and
690 rainfall characteristics on observed and modeled green roof hydrologic performance.
691 *Ecol. Eng.* 73, 494–508. doi:10.1016/j.ecoleng.2014.09.080

692 Hargreaves, G.H., Samani, Z.A., 1985. Reference crop evapotranspiration from ambient
693 air temperature. *Appl. Eng. Agric.* 1, 96–99.

694 Hargreaves, G.L., Hargreaves, G.H., Riley, J.P., 1985. Irrigation Water Requirements for
695 Senegal River Basin. *J. Irrig. Drain. Eng.* 111, 265–275. doi:10.1061/(ASCE)0733-
696 9437(1985)111:3(265)

697 Hilten, R.N., Lawrence, T.M., Tollner, E.W., 2008. Modeling stormwater runoff from
698 green roofs with HYDRUS-1D. *J. Hydrol.* 358, 288–293.
699 doi:10.1016/j.jhydrol.2008.06.010

700 Hutchinson, D., Abrams, P., Retzlaff, R., Liptan, T., 2003. Stormwater monitoring two
701 ecoroofs in Portland, Oregon, USA, *Greening Rooftops for Sustainable*
702 *Communities.*

703 Ippisch, O., Vogel, H.J., Bastian, P., 2006. Validity limits for the van Genuchten-Mualem

704 model and implications for parameter estimation and numerical simulation. *Adv.*
705 *Water Resour.* 29, 1780–1789. doi:10.1016/j.advwatres.2005.12.011

706 Jarrett, a., Hunt, W., Berghage, R., 2006. Annual and individual storm green roof
707 stormwater response models, in: ASABE Annual International Meeting. Portland,
708 Oregon, pp. 1–11.

709 Kasmin, H., Stovin, V.R., Hathway, E.A., 2010. Towards a generic rainfall-runoff model
710 for green roofs. *Water Sci. Technol.* 62(4), 898–905. doi:10.2166/wst.2010.352

711 Krebs, G., Kokkonen, T., Valtanen, M., Setälä, H., Koivusalo, H., 2014. Spatial resolution
712 considerations for urban hydrological modelling. *J. Hydrol.* 512, 482–497.
713 doi:10.1016/j.jhydrol.2014.03.013

714 Kurtz Tim, 2008. Flow monitoring of three ecoroofs in Portland, Oregon. *Low Impact*
715 *Dev. Urban Ecosyst. Habitat Prot.* 11, 1–10. doi:10.1061/41009(333)10z

716 Lamera, C., Becciu, G., Rulli, M.C., Rosso, R., 2014. Green roofs effects on the urban
717 water cycle components. *Procedia Eng.* 70, 988–997.
718 doi:10.1016/j.proeng.2014.02.110

719 Li, Y., Babcock, R.W., 2014. Green roof hydrologic performance and modeling: A
720 review. *Water Sci. Technol.* 69, 727–738. doi:10.2166/wst.2013.770

721 Liu, K.K.Y., Minor, J., 2005. Performance Evaluation of an Extensive Green Roof, third
722 Annual International greening rooftops for sustainable Communities, in:
723 Conference, Awards & Trade Show. Washington, DC, pp. 1–11.

724 Locatelli, L., Mark, O., Mikkelsen, P.S., Arnbjerg-Nielsen, K., Bergen Jensen, M.,
725 Binning, P.J., 2014. Modelling of green roof hydrological performance for urban
726 drainage applications. *J. Hydrol.* 519, 3237–3248.
727 doi:10.1016/j.jhydrol.2014.10.030

728 Lucas, W.C., Sample, D.J., 2015. Reducing combined sewer overflows by using outlet
729 controls for Green Stormwater Infrastructure: Case study in Richmond, Virginia. *J.*
730 *Hydrol.* 520, 473–488. doi:10.1016/j.jhydrol.2014.10.029

731 Maglionico, M., Stojkov, I., Conte, A., Bonoli, A., Cipolla, S., 2014. Green Roofs for
732 Sustainable Water Management in Urban Areas, in: ICUD2014, 13th International
733 Conference on Urban Drainage. Sarawak, Malaysia, pp. 1–8.

734 Marasco, D.E., Hunter, B.N., Culligan, P.J., Gaffin, S.R., McGillis, W.R., 2014.
735 Quantifying Evapotranspiration from Urban Green Roofs: A Comparison of
736 Chamber Measurements with Commonly Used Predictive Methods. *Environ. Sci.*
737 *Technol.* 48, 10273–10281. doi:10.1021/es501699h

738 Mentens, J., Raes, D., Hermy, M., 2006. Green roofs as a tool for solving the rainwater
739 runoff problem in the urbanized 21st century? *77*, 217–226.
740 doi:10.1016/j.landurbplan.2005.02.010

741 Moran, A.C., Hunt, W., Smith, J., 2005. Green Roof Hydrologic and Water Quality
742 Performance from Two Field Sites in North Carolina. *Manag. Watersheds Hum. Nat.*
743 *Impacts* 1–12. doi:doi: 10.1061/40763(178)99

744 Moriasi, D.N., Arnold, J.G., Van Liew, M.W., Binger, R.L., Harmel, R.D., Veith, T.L.,
745 2007. Model evaluation guidelines for systematic quantification of accuracy in
746 watershed simulations. *Trans. ASABE* 50, 885–900. doi:10.13031/2013.23153

747 Mrowiec, M., Malmur, R., Deska, I., 2014. Reduction of Stormwater Volume Using
748 Improved Infiltration Basin i, 1–8.

749 Nash, J.E., Sutcliffe, J.V., 1970. River flow forecasting through conceptual models part I
750 — A discussion of principles. *J. Hydrol.* 10, 282–290. doi:10.1016/0022-
751 1694(70)90255-6

752 Nawaz, R., McDonald, A., Postoyko, S., 2015. Hydrological performance of a full-scale
753 extensive green roof located in a temperate climate. *Ecol. Eng.* 82, 66–80.
754 doi:10.1016/j.ecoleng.2014.11.061

755 Palla, A., Gnecco, I., 2015. Hydrologic modeling of Low Impact Development systems
756 at the urban catchment scale. *J. Hydrol.* 528, 361–368.
757 doi:http://dx.doi.org/10.1016/j.jhydrol.2015.06.050

758 Palla, A., Gnecco, I., Lanza, L.G., 2012. Compared performance of a conceptual and a
759 mechanistic hydrologic models of a green roof. *Hydrol. Process.* 26, 73–84.
760 doi:10.1002/hyp.8112

761 Palla, A., Gnecco, I., Lanza, L.G., 2010. Hydrologic Restoration in the Urban
762 Environment Using Green Roofs. *Water* 2, 140–154. doi:10.3390/w2020140

763 Poë, S., Stovin, V., Berretta, C., 2015. Parameters influencing the regeneration of a green
764 roof's retention capacity via evapotranspiration. *J. Hydrol.* 523, 356–367.
765 doi:10.1016/j.jhydrol.2015.02.002

766 Qin, H., Li, Z., Fu, G., 2013. The effects of low impact development on urban fl ooding
767 under different rainfall characteristics. *J. Environ. Manage.* 129, 577–585.
768 doi:10.1016/j.jenvman.2013.08.026

769 Raimondo, F., Trifilò, P., Lo Gullo, M.A., Andri, S., Savi, T., Nardini, A., 2015. Plant
770 performance on Mediterranean green roofs: interaction of species-specific hydraulic
771 strategies and substrate water relations. *AoB Plants* 7, 1–12.
772 doi:10.1093/aobpla/plv007

773 Rossman, L., 2016. Storm Water Management Model Reference Manual Volume I –
774 Hydrology I.

775 Rossman, L., 2015. Storm Water Management Model Reference Manual Volume I –

776 Hydrology, I.

777 Rossman, L. a., 2010. Storm Water Management Model User's Manual, Version 5.0.

778 United States Environ. Prot. Agency.

779 Savi, T., Andri, S., Nardini, A., 2013. Impact of different green roof layering on plant

780 water status and drought survival. *Ecol. Eng.* 57, 188–196.

781 doi:10.1016/j.ecoleng.2013.04.048

782 She, N., Pang, J., 2010. Physically Based Green Roof Model. *J. Hydrol. Eng.* 6, 458–464.

783 Speak, A.F., Rothwell, J.J., Lindley, S.J., Smith, C.L., 2013. Rainwater runoff retention

784 on an aged intensive green roof. *Sci. Total Environ. J.* 461-462, 28–38.

785 doi:10.1016/j.scitotenv.2013.04.085

786 Spolek, G., 2008. Performance monitoring of three ecoroofs in Portland, Oregon. *Urban*

787 *Ecosyst.* 11, 349–359. doi:10.1007/s11252-008-0061-z

788 Stovin, V., 2010. The potential of green roofs to manage Urban Stormwater 24, 192–199.

789 doi:10.1111/j.1747-6593.2009.00174.x

790 Stovin, V., Poë, S., Berretta, C., 2013. A modelling study of long term green roof

791 retention performance. *J. Environ. Manage.* 131, 206–215.

792 doi:10.1016/j.jenvman.2013.09.026

793 Stovin, V., Poë, S., De-Ville, S., Berretta, C., 2015. The influence of substrate and

794 vegetation configuration on green roof hydrological performance. *Ecol. Eng.* 85,

795 159–172. doi:10.1016/j.ecoleng.2015.09.076

796 Stovin, V., Vesuviano, G., Kasmin, H., 2012. The hydrological performance of a green

797 roof test bed under UK climatic conditions. *J. Hydrol.* 414-415, 148–161.

798 doi:10.1016/j.jhydrol.2011.10.022

799 Teemusk, A., Mander, Ü., 2010. Temperature regime of planted roofs compared with

800 conventional roofing systems 36, 91–95. doi:10.1016/j.ecoleng.2009.09.009

801 Teemusk, A., Mander, Ü., 2007. Rainwater runoff quantity and quality performance from
802 a greenroof: The effects of short-term events. *Ecol. Eng.* 0, 271–277.
803 doi:10.1016/j.ecoleng.2007.01.009

804 Toreti, A., Desiato, F., Fioravanti, G., Perconti, W., 2010. Seasonal temperatures over
805 Italy and their relationship with low-frequency atmospheric circulation patterns.
806 *Clim. Change* 99, 211–227. doi:10.1007/s10584-009-9640-0

807 UNI EN 13041 [WWW Document], 2012. URL [http://store.uni.com/magento-](http://store.uni.com/magento-1.4.0.1/index.php/uni-en-13041-2012.html)
808 [1.4.0.1/index.php/uni-en-13041-2012.html](http://store.uni.com/magento-1.4.0.1/index.php/uni-en-13041-2012.html)

809 Vanwoert, N.D., Rowe, D.B., Andresen, J.A., Rugh, C.L., Fernandez, R.T., Xiao, L.,
810 2005. Green Roof Stormwater Retention: Effects of Roof Surface, Slope, and Media
811 Depth 1044, 1036–1044. doi:10.2134/jeq2004.0364

812 Versini, P. -a., Ramier, D., Berthier, E., de Gouvello, B., 2015. Assessment of the
813 hydrological impacts of green roof: From building scale to basin scale. *J. Hydrol.*
814 524, 562–575. doi:10.1016/j.jhydrol.2015.03.020

815 Vijayaraghavan, K., 2016. Green roofs: A critical review on the role of components,
816 benefits, limitations and trends. *Renew. Sustain. Energy Rev.* 57, 740–752.
817 doi:10.1016/j.rser.2015.12.119

818 Voyde, E., Fassman, E., Simcock, R., 2010a. Hydrology of an extensive living roof under
819 sub-tropical climate conditions in Auckland , New Zealand. *J. Hydrol.* 394, 384–
820 395. doi:10.1016/j.jhydrol.2010.09.013

821 Voyde, E., Fassman, E., Simcock, R., Wells, J., 2010b. Quantifying Evapotranspiration
822 Rates for New Zealand Green Roofs. *J. Hydrol. Eng.* 15, 395–403.
823 doi:10.1061/(ASCE)HE.1943-5584.0000141

824 Yang, W., Li, D., Sun, T., Ni, G., 2014. Saturation-excess and infiltration-excess runoff
825 on green roofs. *Ecol. Eng.* 74, 327–336. doi:10.1016/j.ecoleng.2014.10.023
826 Zhang, S., Guo, Y., 2014. SWMM Simulation of the Storm Water Volume Control
827 Performance of Permeable Pavement Systems. *J. Hydrol. Eng.* 06014010, 431–438.
828 doi:10.1061/(ASCE)HE
829